

## Supplementary Information

Regulation of forward and backward locomotion through intersegmental feedback circuits in *Drosophila* larvae

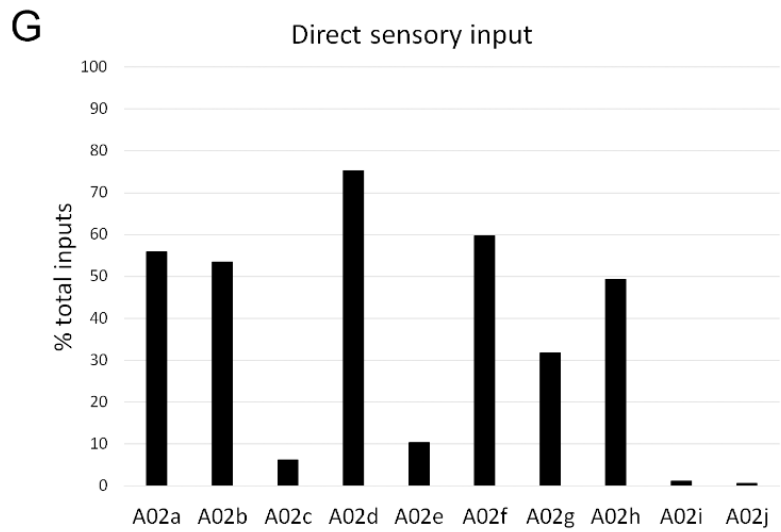
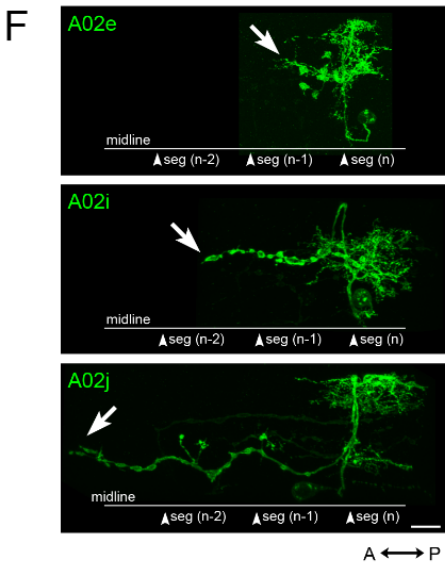
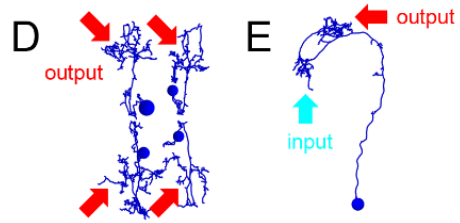
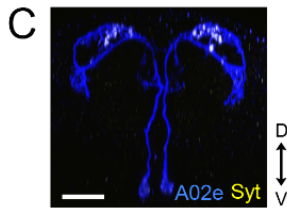
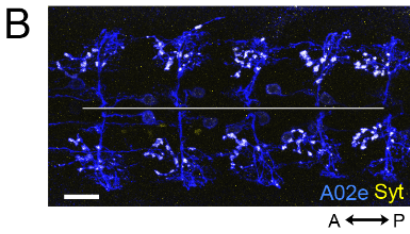
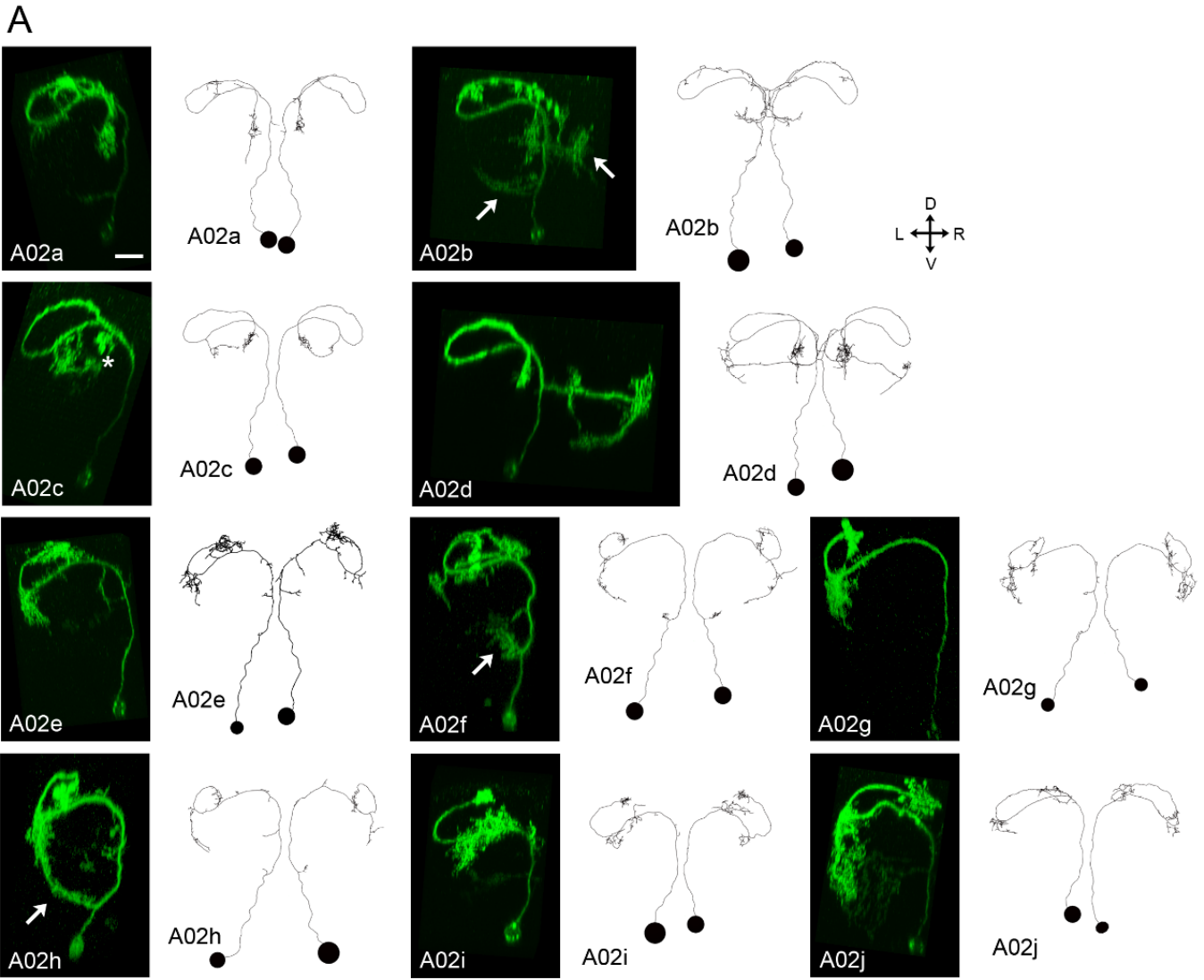
Kohsaka et al.

## Supplementary Methods

### Circuit mapping of PMSIs from EM

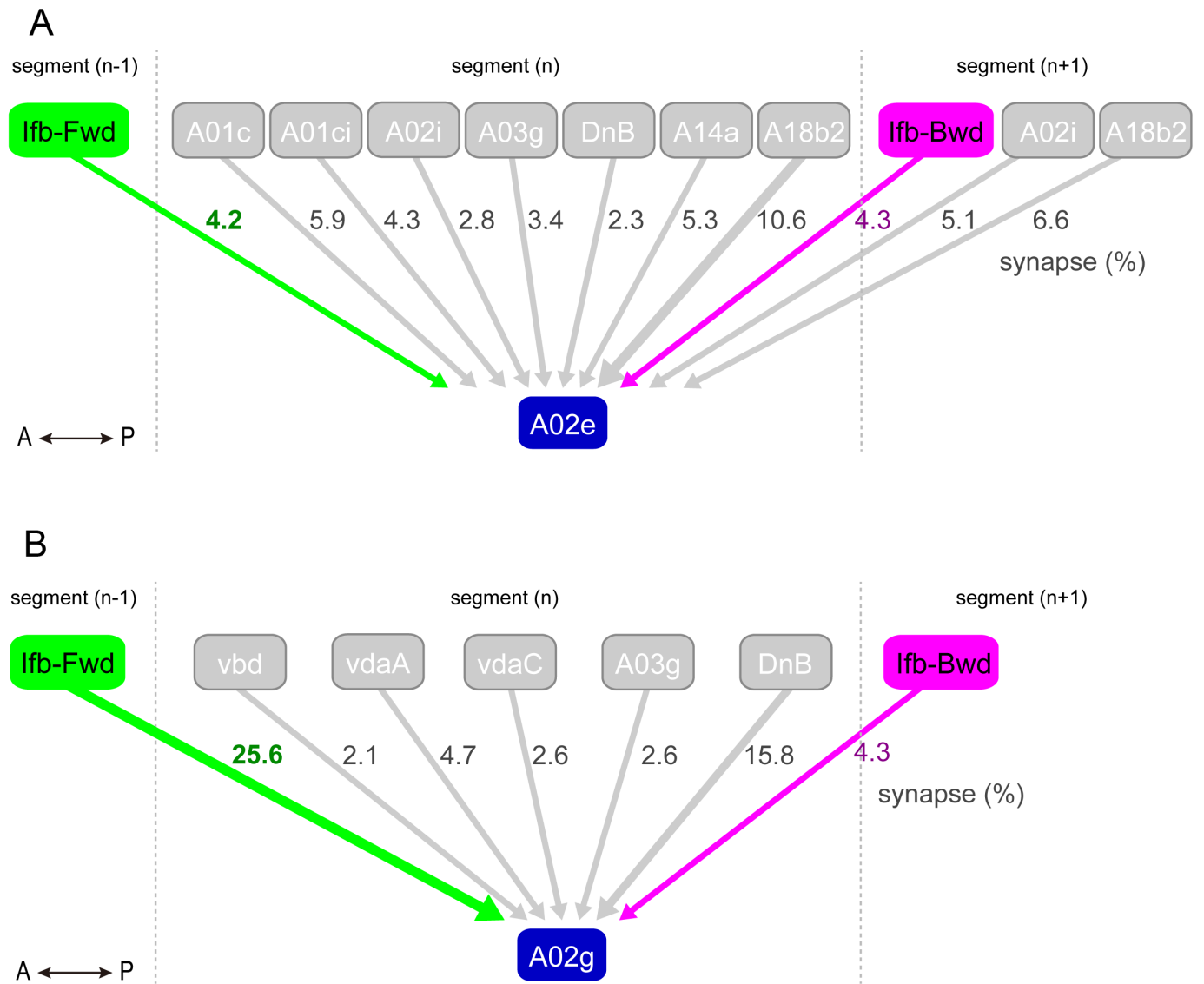
We first reconstructed candidate PMSI neurons in the ssTEM images and compared them to confocal images obtained by clonal analysis (Supplementary Fig. 1A) of each of the ten PMSIs in each hemi-neuromere. The same set of interneurons (termed A02a to A02j<sup>1</sup>) was identified to be present in the neuron reconstruction from EM, based on the soma location, neurite arborization, and position of presynaptic sites (Supplementary Fig. 1A). In the neuron reconstruction from EM, no further neurons possessing axon projections characteristic of PMSIs appeared, suggesting that there are no missing or unanalyzed PMSI neurons. Of the ten PMSIs, we focused our analysis on two, A02e and A02g, which form synapses to MNs locally in the same segment (Supplementary Fig. 1B – 1F, and data not shown) and receive few afferent sensory inputs (Supplementary Fig. 1G) and thus are largely innervated by the 2<sup>nd</sup> order premotor neurons. We excluded the other PMSIs from further analysis since they form synapses to MNs intersegmentally (A02i and j), and do not form synapses to MNs (A02c) or receive major inputs from sensory neurons (A02a, b, d, f and h) (Supplementary Fig. 1).

We next reconstructed the presynaptic neurons of A02e and A02g, and identified eleven and seven major presynaptic interneurons respectively (Fig. 1E, 1F and Supplementary Fig. 2). We reasoned that key upstream neurons regulating multiple 1<sup>st</sup> order premotor neurons would innervate both A02e and A02g. We therefore focused on two common presynaptic neurons, lfb-Fwd (A01d3 in a lineage-based nomenclature) and lfb-Bwd (A27k in a lineage-based nomenclature) (Fig. 1G and 1H), in this study. The other common presynaptic neuron, DnB (Down and back<sup>2</sup>) was excluded because it was not active during fictive locomotion and thus is unlikely to be involved in its regulation (forward waves: n=5 events; backward waves: n=8 events).

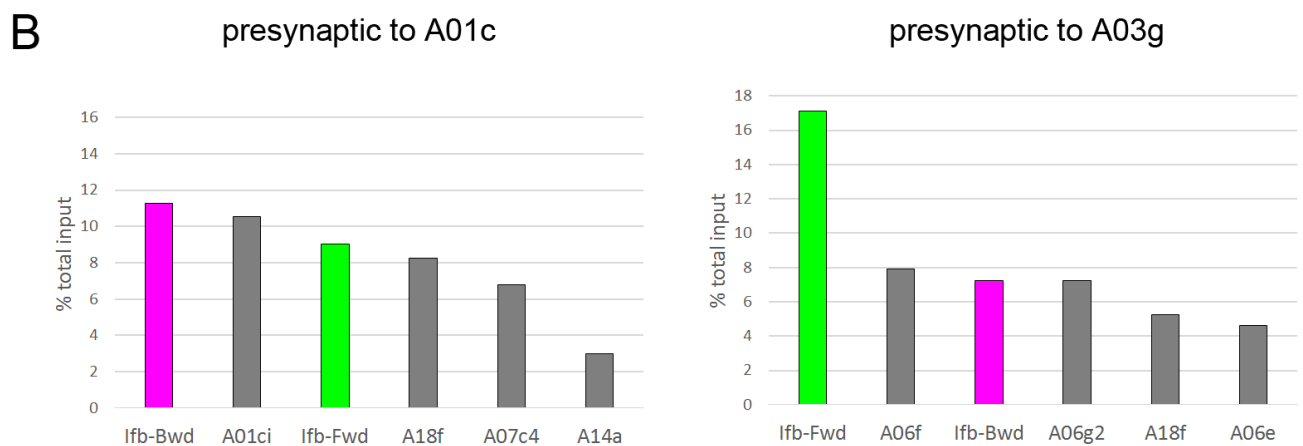
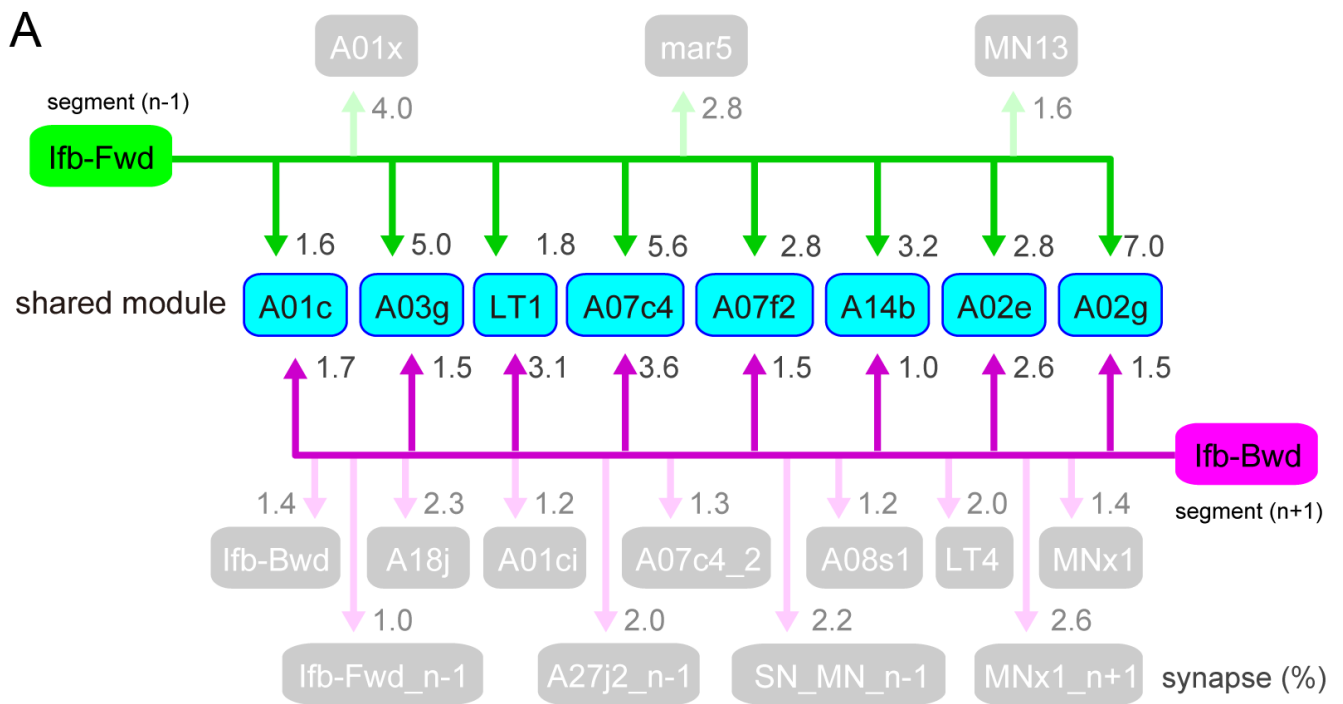


### Supplementary Figure 1. Single cell analysis of PMSIs

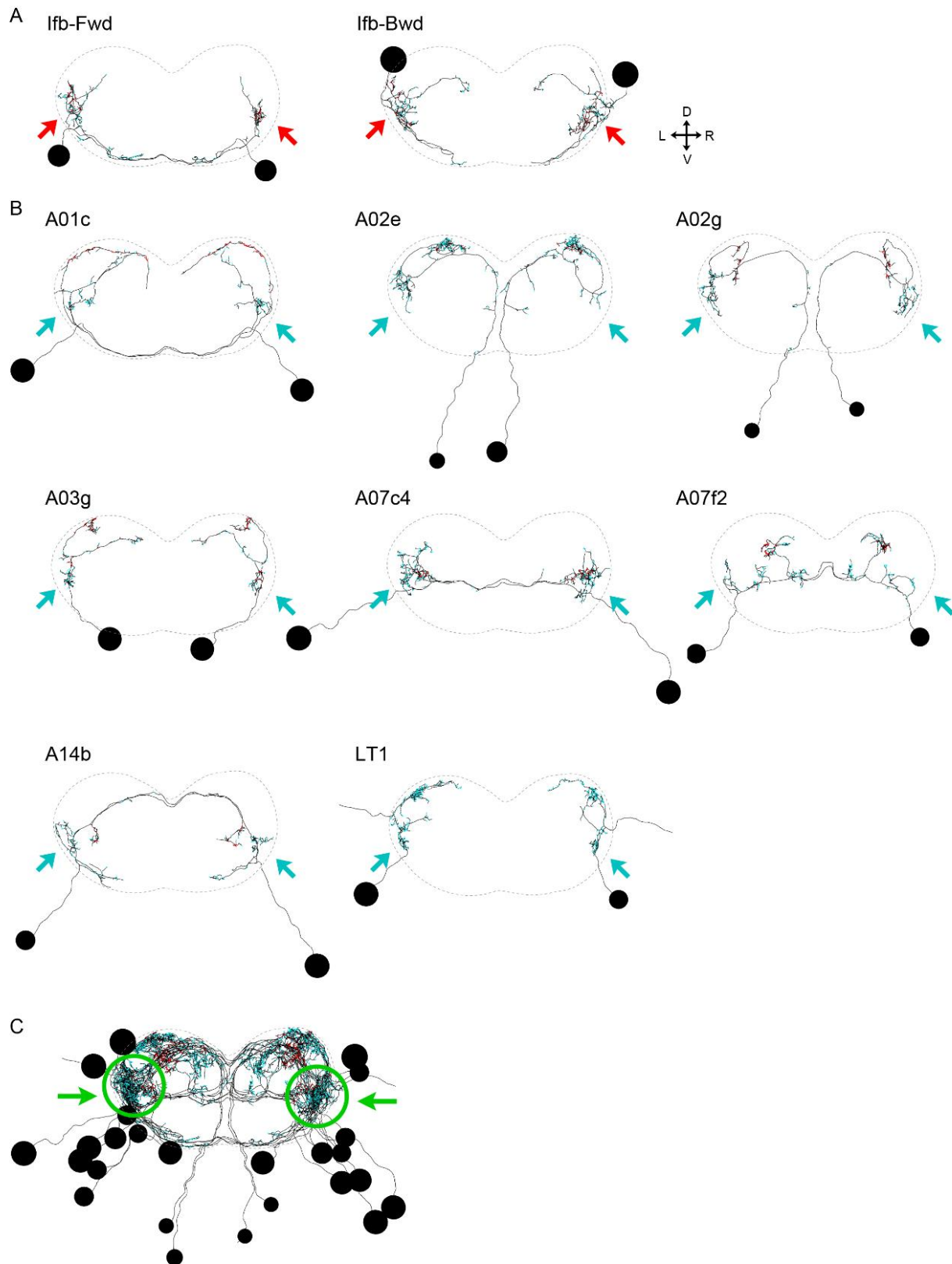
(A) Single cell images of PMSIs (A02a – A02j) by light microscope (left), and neuron reconstruction from EM in posterior view. The light microscope images were obtained by clonal analyses using *period-Gal4 > MCFO*. Putative dendrite location receiving direct sensory projections is shown by arrows. The asterisk shows the presynaptic terminals of A02c, where few motor neuronal dendrites are targeted, indicating that A02c does not innervate MNs directly. (B and C) Dorsal (B) and posterior (C) views of *SS01817 > Syt-HA* CNS showing the neurites (blue) and presynaptic sites (yellow) of a PMSI, A02e (n=2 larvae). (D and E) Dorsal (D) and posterior (E) views of the location of synaptic inputs and outputs in A02e. Note that the location of the output sites is consistent with that of the presynaptic marker in (B) and (C). (F) Dorsal views of light microscope images of A02e, A02i and A02j. The location of TP1 projection<sup>3</sup> in each segment is shown by an arrowhead with relative segmental number as segmental position marker. The tips of presynaptic terminals shown by arrows indicate that A02i and A02j target neighboring segments. (G) The fraction of direct inputs onto PMSIs (A02a - A02j) from somatosensory neurons in the body wall. The fractions are small in A02c, e, g, l and j. Scale bar, 10  $\mu\text{m}$  (A and F) and 20  $\mu\text{m}$  (B and C).



**Supplementary Figure 2. Circuit mapping of presynaptic partners of PMSIs, A02e and A02g from EM**  
Major presynaptic partners (occupying more than 2% of total presynapses) of A02e (A) and A02g (B) are shown. Numbers on arrows indicate the fraction of synapse numbers to total synapses onto A02e (A) and A02g (B).



**Supplementary Figure 3. Circuit mapping of postsynaptic partners of lfb-Fwd and lfb-Bwd from EM**  
 (A) Major postsynaptic partners (occupying more than 1% of total postsynapses) of lfb-Fwd and lfb-Bwd are shown. Numbers on arrows indicate the fraction of synapse numbers to total synapses from lfb-Fwd (on green arrows) and lfb-Bwd (on purple arrows). Several postsynaptic neurons reside in the neighboring segments indicated by “n-1” (anterior next segment) or “n+1” (posterior next segment). The other neurons are located at segment n. Shared neurons are shown in blue. (B) The fraction of inputs onto A01c (left) and A03g (right). The top 6 presynaptic partners to A01c and A03g are shown.



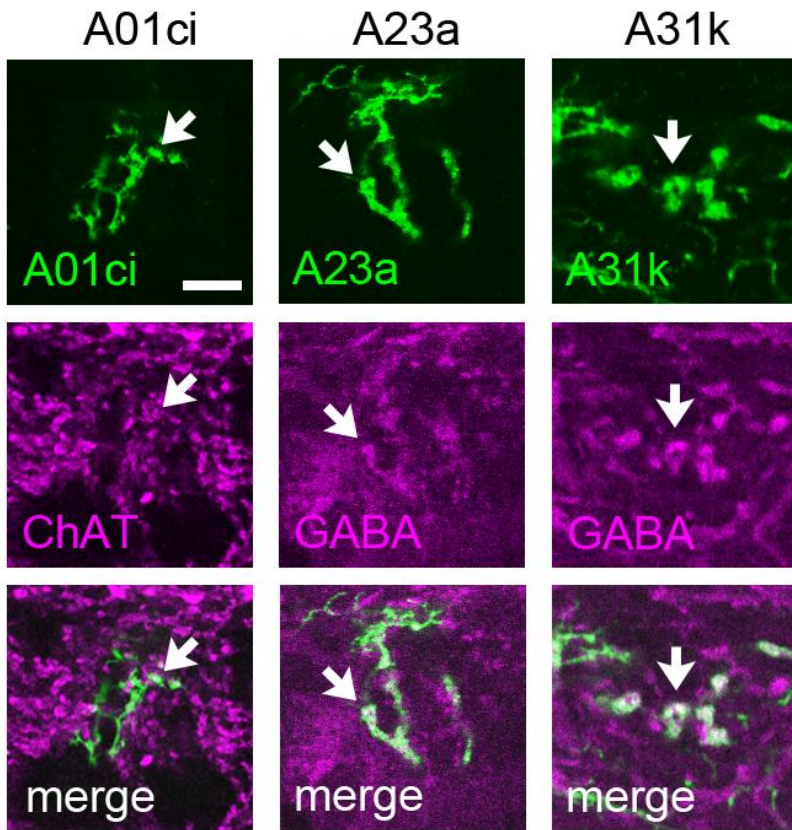
**Supplementary Figure 4. Reconstructed images of the lfb neurons and the shared module neurons**  
 (A and B) Posterior views of the reconstructed lfb-Fwd and lfb-Bwd (A) and the shared module neurons (B). Arrows indicate the presynaptic sites of lfb neurons (red) and the postsynaptic sites of the shared module neurons (blue). (C) Overlay image of lfb neurons (A) and the shared module neurons (B). The presynaptic sites of lfb neurons and the postsynaptic sites of the shared module neurons are accumulated at the centrolateral region of the neuropil (green open circles and arrows).

		A01c	A01ci	A03g	A02e	A02g	A23a	A31k	
Longitudinal-MNs	aCC						24	49	
	U1						45	60	
	U2				9		38	93	
	U5				11			23	
	ISN-MN(1)							27	
	ISN-MN(2)			16				37	
	MN20	22							
	RP2							47	
	RP3				8				
	RP5				15	6			
	RP1				32	32			
	RP4				22	34			
	MN27	14	11	8					
	LO1						15		
	Transverse-MNs	LT1	49	26	19				
LT2		35	15	12					
LT3		37	32	8					Ach (excitatory)
LT4		29	17	8					GABA (inhibitory)
MN18		15		8					Glu (inhibitory)
INs	A01c		14						
	A01ci	17							
	A02e	23	29	20					
	A02g			9					
	A03a5			9					
	A03d/e							6	
	A05k							16	
	A06e			8					
	A06f			12					
	A18j	2	13						
	A19f	3	6						
	A19l			26					
	A23a			8					
	A27j		4						
	A31k			62					
DL2							14		
		A01c	A01ci	A03g	A02e	A02g	A23a	A31k	

**Supplementary Figure 5. Sheet of downstream connectivity of the shared module.**

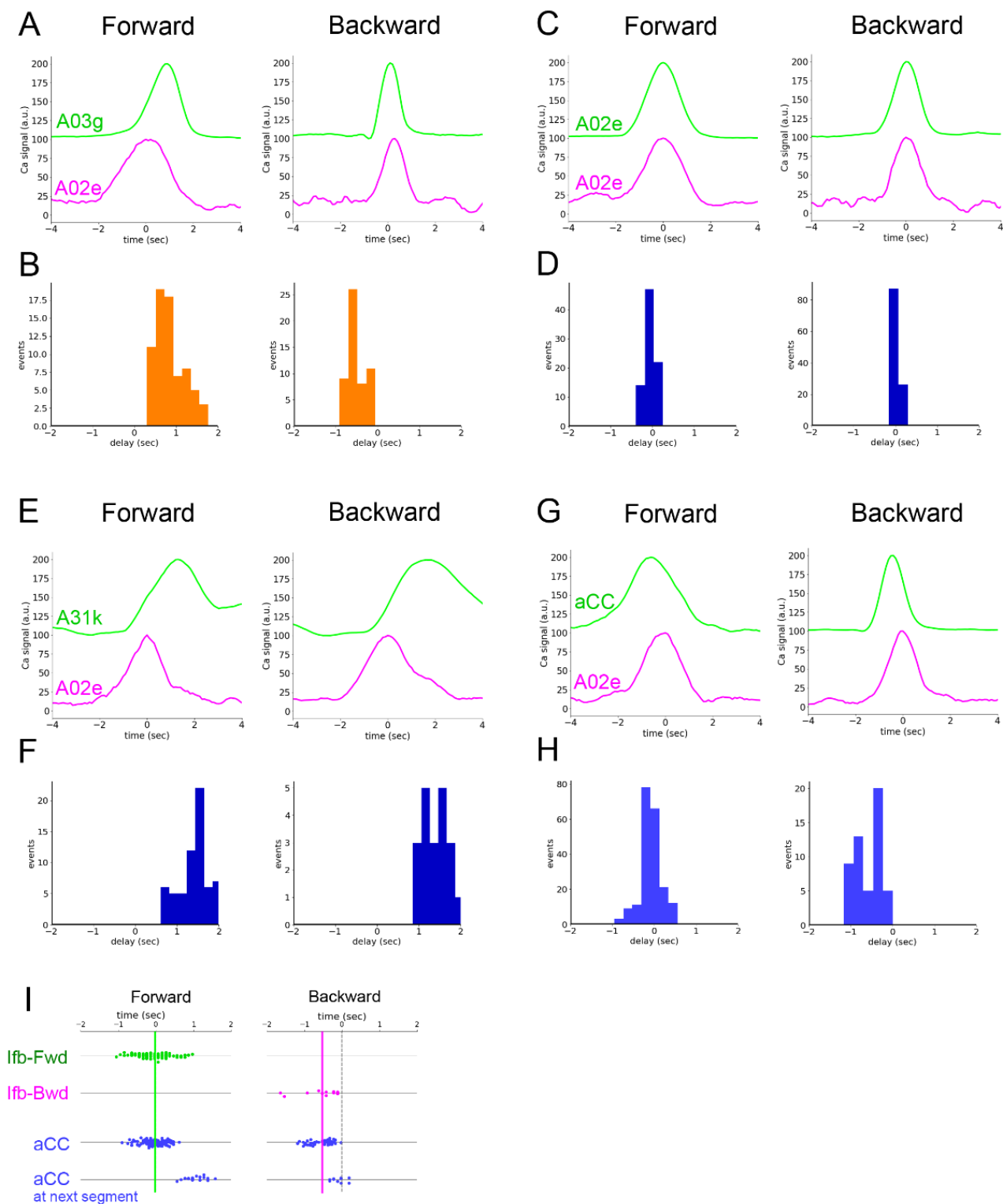
The numbers of postsynaptic sites of the shared module (A01c, A01ci, A03g, A02e, A02g, A23a, and A31k) are shown in each column. The downstream MNs are grouped by the class of target muscles (longitudinal or transverse). Cells in the spreadsheet indicating the connection between the shared neurons and MNs are colored based on the neurotransmitter of the shared neurons.





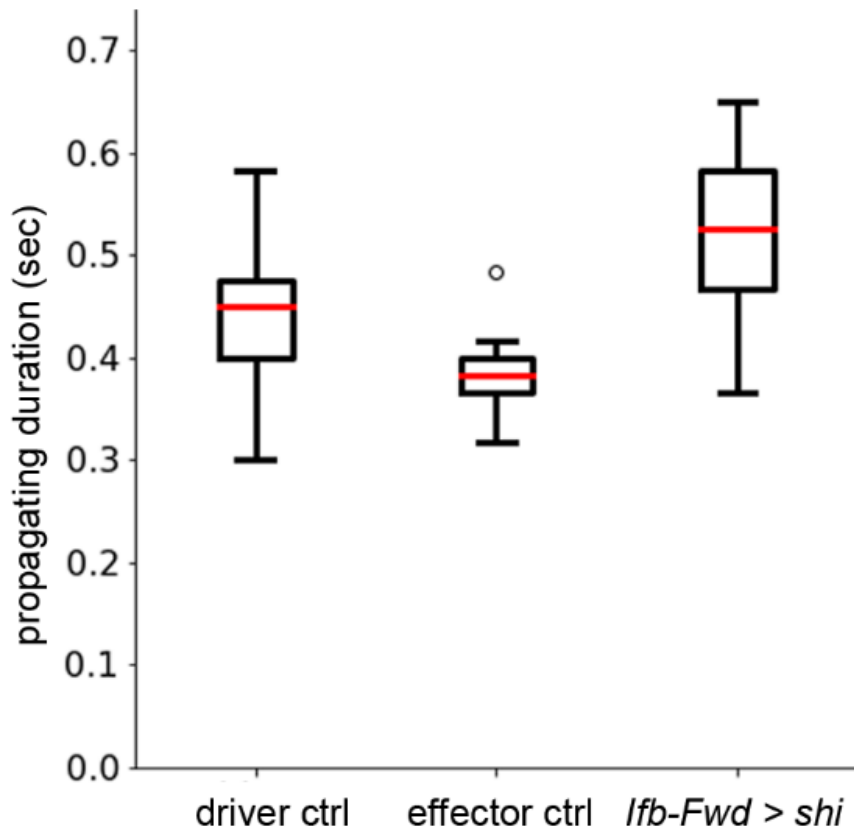
**Supplementary Figure 6. Neurotransmitters of the shared neurons.**

Dorsal view of A01ci (left; *R75H04 > mCD8::GFP*), A23a (middle; *SS04495 > mCD8::GFP*) and A31k (right; *SS04399 > mCD8::GFP*) counterstained for ChAT (left) and GABA (middle and right) (n=2-4 larvae for each neuron). Scale bar, 5  $\mu$ m.



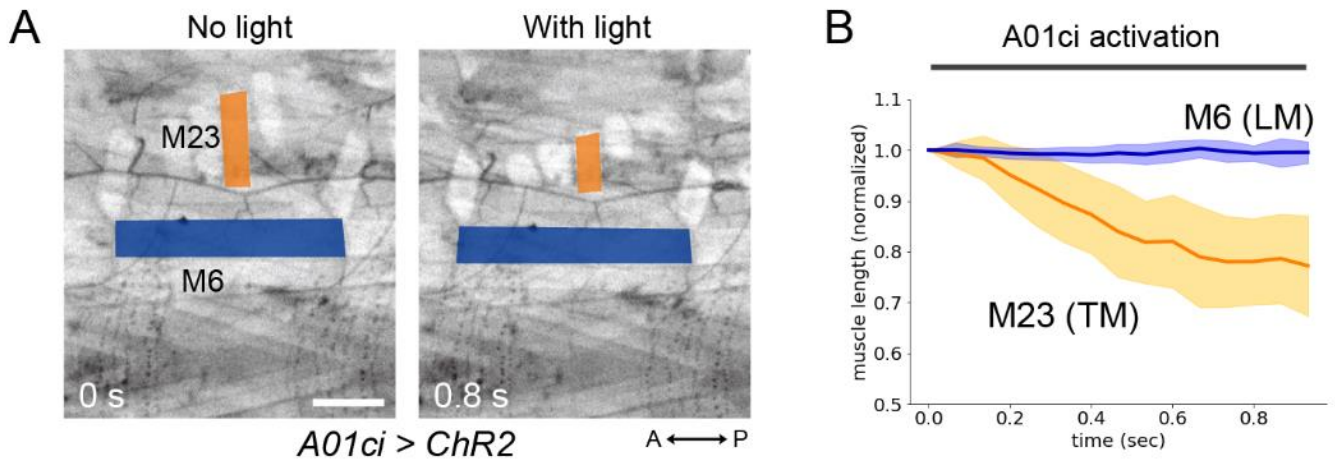
### Supplementary Figure 7. Dual color calcium imaging of the shared module.

(A, C, E and G) Example traces obtained from dual color calcium imaging of A03g (A, green,  $n=6$  larvae), A02e (C, green,  $n=5$  larvae), A31k (E, green,  $n=8$  larvae) and aCC MN (G, green,  $n=14$  larvae) with A02e (magenta) as a reference during forward (left) or backward (right) waves. (B, D, F and H) Histograms of the time delay of the peak activities of A03g (B), A02e (D), A31k (F) or aCC (H) compared to A02e. (I) Scatter plot of activity peaks of aCC MNs in two neighboring segments and lfb neurons during forward and backward waves. The timing of the activity peaks in different neurons was plotted using the A02e activity in a segment as a reference. Average activity peak of lfb-Fwd (in forward propagation) or lfb-Bwd (in backward propagation) was shown by a green or magenta line, respectively.



**Supplementary Figure 8. Inhibition of *lfb-Fwd* neurons with Shibirets decreased the speed of axial propagation of muscle contraction.**

The duration for propagation of muscle contraction from the tail to head was significantly increased by inhibition of *lfb-Fwd* neurons (*lfb-Fwd>shi*,  $0.51 \pm 0.01$  seconds per wave (n=22); driver control,  $0.44 \pm 0.02$  seconds per wave (n=20); effector control,  $0.38 \pm 0.01$  seconds per wave (n=16),  $p=0.003$  (driver control) and  $p=8 \times 10^{-8}$  (effector control) by the two-sided Student's t-test with the Bonferroni correction), which shows that the speed of axial propagation is decreased by inhibition of *lfb-Fwd* neurons. Center line, median; box limits, upper and lower quartiles; whiskers, 1.5x interquartile range; points, outliers.



**Supplementary Figure 9. Optogenetic activation of A01ci.**

(A) Optogenetic activation of A01ci (by *R75H04 > ChR2*) induces contraction of a transverse but not longitudinal muscle. Muscle contraction was imaged by *mhc-GFP*. Scale bar, 100  $\mu\text{m}$ . (B) Quantification of the change in muscle length upon optogenetic activation (indicated by the thick black line at the top,  $n=3$  larvae). Solid lines indicate the mean values and transparent areas mark the standard deviation.

## Supplementary References

1. Schneider-Mizell, C. M. *et al.* Quantitative neuroanatomy for connectomics in *Drosophila*. *Elife* **5**, (2016).
2. Burgos, A. *et al.* Nociceptive interneurons control modular motor pathways to promote escape behavior in *Drosophila*. *eLife* **7**, (2018).
3. Landgraf, M., Sánchez-Soriano, N., Technau, G. M., Urban, J. & Prokop, A. Charting the *Drosophila* neuropile: a strategy for the standardised characterisation of genetically amenable neurites. *Dev. Biol.* **260**, 207–25 (2003).